Atmos. Meas. Tech. Discuss., https://doi.org/10.5194/amt-2018-63
Manuscript under review for journal Atmos. Meas. Tech.
Discussion started: 12 March 2018

Atmospheric Measurement Techniques Discussions
Open Access

Characteristics of vertical velocities estimated from drop size and fall velocity spectra of a Parsivel disdrometer

Dong-Kyun Kim and Chang-Keun Song

School of Urban and Environmental Engineering,
Ulsan National Institute of Science and Technology, Ulsan, Korea

Corresponding Author: Prof. Chang-Keun Song, School of Urban and Environmental Engineering, Ulsan National Institute of Science and Technology, Ulsan, Korea, Email:cksong@unist.ac.kr

Atmos. Meas. Tech. Discuss., https://doi.org/10.5194/amt-2018-63
Manuscript under review for journal Atmos. Meas. Tech.
Discussion started: 12 March 2018

Atmospheric Measurement Techniques Discussions

Abstract

Vertical air velocities were estimated from drop size and fall velocity spectra observed by Parsivel disdrometers during intensive field observations from 13 June to 3 August 2016 around Mt. Jiri (1915 m above sea level) in the southern Korean Peninsula. Rainfall and wind velocity data measured by Parsivel disdrometers and ultrasonic anemometers, respectively, were analyzed for an orographic rainfall event associated with a stationary front over Mt. Jiri on 1 July 2016. In this study, a new technique was developed to estimate vertical air velocities from drop size and fall velocity spectra measured by the Parsivel disdrometers and investigate characteristics of up-/downdrafts and related microphysics in the windward and leeward side of the mountain.

To validate results from this technique, vertical air velocities between the Parsivel and anemometer were compared and were in quite good agreement each other. It was shown that upward motions were relatively more dominant in the windward side and even during periods of heavy rainfall. On the contrast, downward motions were more dominant in the leeward side even when heavy rain occurred. Occurrences of upward and downward motions were digitized as percentage values as they are divided by the total rainfall period. In the windward (leeward) side, the percentages of upward (downward) motion were larger than those of downward (upward) motion. Rainfall intensity in the leeward side was relatively stronger than in the windward side, suggesting that the increase in rainfall in the leeward side was more affected by the downward motions.

Key words: vertical air velocity, drop size spectra, microphysics, Parsivel disdrometer

Atmos. Meas. Tech. Discuss., https://doi.org/10.5194/amt-2018-63
Manuscript under review for journal Atmos. Meas. Tech.
Discussion started: 12 March 2018

Atmospheric Measurement Techniques Discussions

1. Introduction

Drop size distribution (DSD) and related rain parameters from surface disdrometer measurements or indirectly retrieved from remote sensing measurements such as radars, wind profilers, or satellites provides key information for a better understanding of microphysical processes that account for drop growth or decay within precipitating systems. However, DSD uncertainties always exist as its retrieval is vulnerable to various factors such as measurement errors, sampling difference in volume and height, strong winds, up-/downdrafts, turbulence, and so on as have been reported in many previous studies (Jameson and Kostinski 1998; Cao et al., 2008; Tokay et al., 2009; Thurai et al., 2012). Thus a validation of such retrieved DSDs by comparing with those from surface disdrometers is not straightforward (Williams et al. 2000) due to their different environment although minimizing a sampling difference as much as possible is needed. Even if DSDs are accurately obtained, their characteristics, particularly between convective and stratiform rain, can vary largely from small areas in short-time scale to climatic regimes in long-term.

Ground-based classifications of convective, mixed, or stratiform rain type have been performed in various ways such as characteristics in integral DSD parameters (i.e., rain rate, mean drop diameter, etc), bright band signature, vertical gradients in Doppler velocity and reflectivity, vertical draft magnitude, and so on (Atlas et al., 2000; Cifelli et al., 2000; Tokay et al., 1996, 1999; Thurai et al., 2016; Williams et al., 1995). Tokay et al. (1999) classified rainfall types from collocated disdrometer and 915 MHz profiler observations in tropical rain events and indicated that compared to profiler classifications that utilize vertical gradients in Doppler velocity, a disdrometer is relatively more feasible to misclassify stratiform rain as convective or vice versa due to time-height ambiguity mostly associated with advection of drops while falling to the ground.

In measuring and validating surface DSDs, there is no such handy, transportable, and lowcost instrument like disdrometer that has long been used as a ground truth although it has inherent problems mentioned above as exposed to all different environments. Parsivel disdrometer (hereafter Parsivel) is one of disdrometers widely used for DSD studies over the world. As deduced from its name, par-si-vel (particle size and velocity), this disdrometer measures fall velocities, sizes, and number counts of liquid and ice particles falling into 32 (size) x 32 (fall velocity) bins. Parsivel has been used at observatories or in numerous field experiments to examine and validate microphysical properties by comparing DSDs and integral DSD parameters with those from other type disdrometer, 2-Dimentional Video Disdrometer (2DVD) and radar and profiler observations for various events of precipitation (Kim et al., 2010; Thurai et al., 2016).

A Parsivel-measured fall velocity of a raindrop is the sum of a raindrop terminal fall speed (in stagnant air) and vertical air motion. Thus when there are updrafts or downdrafts, the Parsivel-measured fall velocity is deviated from the terminal fall speed even if drop sizes are identical. On top of this, strong horizontal winds, vertical shear, or turbulence can disperse the distribution of drop size and fall velocity, leading to a change (or bias) in the Parsivel-measured fall velocity averaged over the distribution. Consequently, all these factors would affect DSD integral parameters such as rain rate although single or mixed effects of the factors on these have not been fully understood (Niu et al., 2010). Ulbrich (1992) examined errors in rain rate that result from inaccuracies in fall speeds of raindrops (i.e., inaccurate estimation of vertical air motion) and indicated that updraft will result in larger rain rate at a given reflectivity than when there are no vertical winds. Niu et al. (2010) investigated differences in distributions of drop sizes and fall velocities between convective and stratiform rain and ascribed different deviations in Parsivel-measured fall velocities between small and large drops to vertical air motion and turbulence. Parsivel is prone to measurement errors particularly when there are strong winds and turbulence, leading to discrepancies in comparison with other measurements in the same locations. Tokay et al. (2009, 2014) indicated that the old version of Parsivel tends to underestimate the number of small drops and overestimate drop size larger than 2.0 mm in heavy rain as well as in windy conditions. When they compared each old and new version of Parsivel with Joss-Waldvogel disdrometer and rain gauge measurements, the new version of Parsivel (referred to as Parsivel^2 in their paper) appeared to have a noticeable improvement over the old one for measuring drop size and rainfall rate.

To our knowledge, no studies of vertical air velocities retrieved from Parsivel-measured drop size-fall velocity spectra have been documented or reported yet. In this study we utilize Parsivel and anemometer data collected during intensive field observations that targeted to investigate orographic rainfall mechanisms around mountain areas in the southern region of Korea. A simple technique to retrieve vertical air velocities from Parsivel measurements is developed and first applied to an orographic heavy rain event. This paper is organized as follows. In Section 2, the retrieval technique and instruments used in this study are introduced. A case description about the rain event is followed in Section 3. Results about characteristics of up-/downward motions and related microphysics in the windward and leeward side are presented in Section 4. A summary and conclusions follow in Section 5.

2. Instrumentation and method

Two main instruments used in this study are Parsivel disdrometer and ultrasonic anemometer collocated at three different stations around Mt. Jiri (see Figure 1). Their data were collected during the intensive observation period from 13 June to 3 August 2016 to cover a summer rainy season which is called "Changma" in Korea were analyzed. Parsivel disdrometer (Parsivel), manufactured by OTT (Germany), uses laser-optical properties to measure both sizes and fall velocities of precipitation particles and derives quantities of radar reflectivity, precipitation intensity, etc from measured drop spectra. Time resolution is 1 min. For more details about Parsivel, please see the Löffler-Mang and Joss (2000)'s paper. The ultrasonic anemometer (hereafter UVW) measures east-west (u), north-south (v), and vertical (w) components of winds by using the speed of sound moving along winds between the three nonorthogonal sonic axes and generates wind speed and direction at 1-min interval. The w component observed by UVW is referred to as w_{UVW}.

In this study, a simple, new scheme to derive vertical air velocity (w) from Parsivel measurements is developed by using a relationship of Atlas et al. (1973) between terminal fall velocities and drop diameters in still air as shown by

$$V_f = 9.65\text{-}10.43{*}\exp(\text{-}0.6D), \tag{1}$$

where D is drop diameter in mm and V_f is terminal fall velocity (m s^{-1}) and also the vertical relation of air as shown below

$$w = V_p - V_f\,(\rho_0/\rho)^{0.4} \tag{2}$$

where V_p is Parsivel-measured fall velocity averaged over 32 diameter classes in a size and velocity spectrum and $(\rho_0/\rho)^{0.4}$, where ρ is air density (kg m^{-3}) parameterized by $\rho(z)= \rho_0\exp(-z/9.58)$ and z is altitude in kilometers, is the term that corrects V_f in relation to atmospheric density (Beard 1985) since V_f increases as atmospheric density decreases exponentially with height. In all the terms, negative means downward. The atmospheric density correction was applied to calculate w although the altitudes of D1, D2, and D4 are relatively low at 105, 280 and 313 m AGL, respectively. Thus a mean w value at 1-min interval is finally estimated by subtracting V_p from V_f calculated from Eq (1). The final w estimate is hereafter called w_{par}. For more details, please see the flowchart in Figure 2 that shows how w is estimated from a 1-min drop size (D) and fall velocity (V_p) spectrum of Parsivel. Figure 3 illustrates three conditions of determining zero w, upward w, or downward w value for given size and fall velocity spectra. For the case 1, w would be zero since the D-V_p distribution closely follows the V_f line. Upward w value is determined for the case 2 that V_p is smaller than V_f (i.e., the distribution is towards below the V_f line). For the case 3, downward w value is determined since V_p is larger than V_f. For w_{par} validation, w_{par} is compared with w_{UVW} and its result is described in Section 4.

3. Case description

During a summer rainy season usually from late June to mid July in Korea, severe weather phenomena accompanied by heavy rainfall often occur in the southern region of the Korean Peninsula mostly covered by complex high mountains. In association with terrain-induced up-/downdrafts, mountainous areas can play an important role in controlling formation, amount, and distribution of rainfall. As precipitation systems move over these areas, they tend to develop rapidly and produce localized heavy rainfall. Observational analysis from radar and surface measurements in these areas is necessary to understand terrain effects on rainfall development and microphysics. Thus we performed intensive field observations around Mt. Jiri (1915 m ASL) during the 2016 summertime in the southern Korean Peninsula.

During the observation period of 13 June~3 August 2016, several rain events were observed. On 1 July 2016, a rainfall system associated with a Changma front has developed over the West Sea and moved towards Mt. Jiri. As it passes over the mountain from the east, heavy rainfall was produced and observed by Parsivel disdrometers and UVWs from 1200 to 2200 UTC. Also a dual-Doppler radar analysis (Liou et al., 2012) was also conducted to obtain 3-D wind components from radial velocity data of two Doppler radars as well as vertical structure of radar reflectivity in this mountain area. Figure 4 shows a daily accumulated rainfall distribution and topography of Mt. Jiri. Large rainfall up to 90 mm was seen around the top and south of Mt. Jiri. This is related to more moist upwind flows in the windward side closer to the ocean.

4. Results

4.1. w comparison in time series

For the w_{par} validation, the observed w_{UVW} is compared at time series. Time series of radar reflectivity (Z), rain rate (R), mass-weighted mean diameter (D_m) measured from Parsivel are also examined together. As shown in Fig. 4, three stations of D1, D2, and D4 where both the Parsivel and UVW data are available were selected out of total nine stations. D1 and D2 are windward and D4 is leeward of Mt. Jiri. Figure 5 shows the time series of Z, R, and D_m (left) and w (right) between the Parsivel and UVW observed at D1, D2, and D4. At D1 and D2, high values of Z > 40 dBZ and R > 20 mm h^{-1} are observed during the 1230-1330 UTC period and at around 1730 UTC in Figs. 5a and b. Correspondingly, large D_m values reaching 2 mm were analyzed in these periods. In Fig. 5c, high Z and R were also observed in the leeward side but showing a little time lag compared to those in Figs. 5a and b.

It is shown in Figs. 5d, e, and f that w_{par} matches quite well with w_{UVW}. On the windward side (D1, D2), they both show mostly upward motions and importantly, larger upward motions during periods of heavy rainfall (i.e., 1230-1330 UTC and around 1730 UTC). In contrast, downward motions are mostly found on the leeward side. It is noted that there exists relatively large difference between w_{par} and w_{UVW} with the opposite signs during these high R periods in Fig. 5f. The upward biases of w_{par} in these periods are related to the fact that for a given V_f, a mean V_p became smaller in Eq (2) due to an increase of a larger number of drops ranged at 1~3 mm or a scatter of these drops below the V_f line in the D-V_p distribution, to be more like the case 2 in Fig. 3. A physical reason for this is not clear yet but it is probably resulted from strong winds and turbulence during the high R periods. In other periods, they

Atmos. Meas. Tech. Discuss., https://doi.org/10.5194/amt-2018-63
Manuscript under review for journal Atmos. Meas. Tech.
Discussion started: 12 March 2018

Atmospheric Measurement Techniques Discussions

show quite good agreement. Also, the maximum values of w_{par} and w_{UVW} hardly exceed ± 0.5 m s^{-1}, almost the one-fifth of horizontal wind magnitudes (not shown), suggesting that winds are almost horizontal during the analysis period and they just pointed up or downward, depending on w signs and magnitudes. At D1 and D2, the relatively larger w_{par} and w_{UVW} were found during heavy rain with R > 20 mm h^{-1} around 1300 and 1740 UTC (Figs. 5d and e), indicating that updrafts contributed more on the substantial R increase on the windward side. As downward motions were found on the leeward side even during the periods of heavy rain (R > 20 mm h^{-1}) as shown in Fig. 5f, an R increase on the leeward side is more associated with the downward w component of winds.

Figure 6 shows characteristics of Z-R relations at D1, D2, and D4. The upward w_{par} values are colored in red and the downward w_{par} in blue. Also we converted them into percentages by dividing by a total of counts in each class with R > 0.5 mm h^{-1} only. At D1 and D2, they were similar as the percentage for the upward w_{par} class is 61% and 71% and the percentages for downward w_{par} class is 39% and 29%, respectively. In contrast, the upward w_{par} percentage at D4 is 31%, much smaller than that at D1 and D2 as found in Fig. 5, and the downward w_{par} percentage is 69%. It is also important to see subtle changes in a coefficient α and exponent β in a Z-R power law form of $Z=\alpha R^{\beta}$. There was a decrease in α from D1 and D2 (250, 252) on the windward side to D4 (226) on the leeward side and a slight increase in β from D1 and D2 (1.31, 1.39) to D4 (1.43). This makes the Z-R line less steep and thus for a given Z, R is larger at D4 than D1 or D2, indicating that rainfall are relatively more strong at D4.

4.2. Histogram analyses

4.2.1 w histograms with regard to R

The w_{par} and w_{UVW} time series discussed in Section 4.1 are examined in their histograms with regard to R. In this study, stratiform and convective rain was simply classified by a threshold of R < 10 mm h^{-1} and R > 10 mm h^{-1}, respectively, which has been often used in previous DSD studies (Leary and Houze 1979). In Figs. 7a, b, c, the w_{par} histograms showed overall agreement with the w_{UVW} at all stations and relatively, the better agreement was found in the stratiform class (R < 10 mm h^{-1}) than the convective class. D1 and D2 showed the quite similar histograms of w_{par}, compared to D4. At D1 and D2, all convective rain has occurred almost in association with upward motions, while for stratiform rain, it occurred with both upward and downward motions (Figs, 7a and b). Importantly, almost the half or a little larger portion of stratiform rain has occurred in association with upward motions. In contrast, at D4, most of stratiform rain was associated with downward motions and convective rain was associated with both upward and downward motions (Fig. 7c). In other words, the latter indicates that heavy rainfall on the leeward side was relatively more associated with downward motions than on the windward side (D1, D2) as noted in the previous section. Figures 7d,e,f show the areas occupied by the upward and downward w values in percentage at each station, same as those shown in the Z-R scatterplots in Fig. 6. Dominant w class is easily seen by these percentage values at each station. In the downward w group, the largest percentage (69%) is found at D4 (Fig. 7f).

4.2.2 Characteristics of Z histograms with regard to w and R

The w_{par} properties discussed in Section 4.1 are examined by Z histograms with regard to w and R. In Fig. 8a, a much larger percentage (61%) in the upward w group is found at D1 showing a relatively wider Z distribution, compared to that at D4 in Fig. 8d. In Fig. 8b, the R percentage classified as convective was 9%, much smaller than 61% in the upward w group in Fig. 8a, suggesting that 52% of the upward w group was associated with stratiform rain. In order to study such relationships between w and R, histograms were split by four conditions in the upper-right corner shown in Figs. 8c and f. That is, each group of R > 10 mm h^{-1} and R < 10 mm hr^{-1}, which is regarded as convective and stratiform rain, respectively, is separated by upward and downward w. Therefore, for instance, 91% of the group R > 10 mm h^{-1} in Fig. 8c is equal to the sum of 52% of the upward w and 39% of the downward w group. Likewise, the upward and downward w group is also split by the two R conditions. Unlike D4, there was no thick blue line at D1 in Fig. 8c because there were no data fell into this category of the downward w and R > 10 mm h^{-1} as shown in Fig. 7a.

In Fig. 8c, convective rain (R > 10 mm h^{-1}) with the largest mean Z has occurred solely in association with upward w motions (thick red line). Among the four categories, the majority percentage of 52% was found in the category of the upward w and R < 10 mm h^{-1} at D1 but 65% was found in the category of the downward w and R < 10 mm h^{-1} at D4. The widest Z distribution were shown in these categories. In Fig. 8d, a much larger percentage is found in the downward w group as noted previously. In Fig. 8e, a larger percentage of 18% is found in the group R > 10 mm h^{-1}, compared to the counterpart (9%) at D1, indicating that on average sense, rain intensity was stronger at D4 (leeward). It is noted that at D4, convective rain has occurred in association with both updrafts (14%) and downdrafts (4%). The little portion of convective rain with relatively smaller Z happened in association with downdrafts. It is thus suggested that downdrafts can play a significant role in increasing R, even larger than 10 mm h^{-1} although the strongest R was related to updrafts rather than downdrafts. Most of stratiform rain was associated with downdrafts (65%).

4.2.3. Histogram characteristics of DSD parameters with regard to w_{par}

In Fig. 9, characteristics of DSD parameters retrieved from the Parsivel measurements are analyzed with regard to w_{par}. Compared to classic DSD retrieval studies without considering w properties, in this study, two histograms split by the upward and downward w were obtained *per* each parameter, which is a first time ever. In Fig. 9b, The Z histograms at D4 show higher Z distributions with mean values of 34.8 and 25.6 dBZ in the upward and downward w category, respectively, are shown, compared to those (25.2 and 18.2 dBZ) at D1 in Fig. 9a. At both D1 and D4, the mean Z, R, and D_m values in the upward w category were higher than those in the downward w category. Between D1 and D4, the mean Z, R, and D_m over the entire data were higher at D4, indicating that rain intensity was somewhat stronger than D1 although the maximum Z (~50 dBZ) and R (below ~60 mm hr^{-1}) were quite similar each other (see the time series of Z and R in Fig. 6). For R, the mean R value of 15.1 mm hr^{-1} was higher at in the upward w group at D4 than 6.22 mm hr^{-1} in the counterpart at D1 (Figs. 9c and g). The mean D_m was largest at 1.37 mm in the upward w category of D4 in Fig. 9f and smallest at 0.86 mm in the downward w category of D1 in Fig. 9b. Thus, the mean D_m (1.03 mm) in the downward w category of D4 was greater than that (0.86 mm) in the same category of D1. This indicates that there were a comparatively larger number of large drops at D4 in association with downward motions which were dominant even during the strong R period. Thus, it is stressed that relative to the windward side, downward motions have more influenced the growth in drop size and increase in R intensity in the leeward side.

5. Summary and conclusions

Intensive field observations around Mt. Jiri for the orographic rainfall events associated with a Changma front in the southern regions of the Korean Peninsula were conducted during summertime in 2016. In order to examine up-/downward w properties in the windward and leeward side of Mt. Jiri, a simple technique was newly developed to retrieve vertical velocities (w) from drop size and fall velocity spectra of the Parsivel disdrometers at different stations. Their comparison with the w-components observed by UVW showed quite good agreement each other, producing the similar histograms between the two instruments. On the

Atmos. Meas. Tech. Discuss., https://doi.org/10.5194/amt-2018-63
Manuscript under review for journal Atmos. Meas. Tech.
Discussion started: 12 March 2018

windward side (D1 and D2), upward motions were more frequently observed and particularly larger upward motions were found during the periods of strong R > 10 mm h^{-1}. For the leeward side (D4), downward motions were more dominant even during the same strong R periods as in the windward side. The downward w percentage was more than a double of the upward w percentage. Importantly, this suggests that strong rain of R > 10 mm hr^{-1} in the leeward side was more associated by negative w-components of winds. Most of stratiform rain also occurred with downward motions. Thus, compared to the windward side where upward motions dominated, downward motions have contributed more on drop growth as well as R increase in the leeward side.

Therefore, the newly developed technique to estimate w values from Parsivel drop size and fall velocity spectra is found physically meaningful and can be applicable to w studies to compare with other w retrievals and investigate their effects on rainfall development in relation to up-/downdrafts aloft especially in orographic regions. The estimated w values showed notably different characteristics in magnitude and signs between the windward side and leeward side during rainfall with dependence on how a size and fall velocity spectrum distributes. Thus, the observed D-V_p distributions appeared to be strongly connected to w properties at surface. In this study, the estimated w values are small in magnitude mostly less than $\pm$0.5 m s^{-1}, almost the one-fifth of horizontal wind magnitudes, indicating that prevailing winds were almost horizontal in this case study.

There was a relatively large difference between w_{par} and w_{UVW} with the opposite signs during these high R periods (Fig. 5f). This is probably associated with strong winds and turbulence that may scatter the D-V_p distribution of drops below the V_f line and further bias w magnitudes. Hence the w retrieval from the disdrometer-based technique is not totally free from environmental conditions. Since the effects of winds and turbulence were not analyzed in this study, we will soon investigate their effects on D-V_p distributions as well as resultant w

biases in a quantitative way as a subsequent work.

Acknowledgements

This research was supported by the National Strategic Project-Fine Particle of the National Research Foundation of Korea(NRF) funded by the Ministry of Science and ICT(MSIT), the Ministry of Environment(ME), and the Ministry of Health and Welfare(MOHW).(NRF-2017M3D8A1092021)

Atmos. Meas. Tech. Discuss., https://doi.org/10.5194/amt-2018-63
Manuscript under review for journal Atmos. Meas. Tech.
Discussion started: 12 March 2018

Atmospheric Measurement Techniques
Discussions

References

Atlas, D., Srivastava, R. C., Sekhon, R. S., 1973. Doppler radar characteristics of precipitation at vertical incidence. Rev. Geophys. Space Phys., 11, 1–35.

Atlas, D., Ulbrich, C. W., Marks, F. D., Black, R. A., Amitai, E., Willis, P. T., Samsury, C. E., 2000. Partitioning tropical oceanic convective and stratiform rains by draft strength. J. Geophys. Res., 105, 2259-2267.

Barnes, G. M., Stossmeister, G. J., 1986. The structure and decay of a rainband in Hurricane Irene (1981). Mon. Wea. Rev., 114, 2590-2601.

Barnes, G. M., Zipser, E. J., Jorgensen, D. P., Marks, F. D., 1983. Mesoscale and convective structure of a hurricane rainband. J. Atmos. Sci., 40, 2125-2137.

Beard, K.V., 1985. Simple altitude adjustments to raindrop velocities for Doppler radar analysis. J. Atmos. Oceanic Technol. 2, 468–471.

Black, M. L., Burpee, R. W., Marks, F. D., 1996. Vertical Motion Characteristics of Tropical Cyclones Determined with Airborne Doppler Radial Velocities. J. Atmos. Sci., 53, 1887–1909.

Brandes, E. A., Zhang, G., Vivekanandan, J., 2004. Comparison of Polarimetric Radar Drop Size Distribution Retrieval Algorithms. J. Atmos. Oceanic Technol., 21, 584–598.

Brandes, E. A., Zhang, G., Vivekanandan, J., 2004. Drop Size Distribution Retrieval with Polarimetric Radar: Model and Application. J. Appl. Meteor., 43, 461–475.

Bringi, V. N., Chandrasekar, V., Hubbert, J., Gorgucci, E., Randeu, W. L., Schoenhuber, M., 2003. Raindrop size distribution in different climatic regimes from disdrometer and dual-polarized radar analysis. J. Atmos. Sci. 60, 354–365.

Bringi, V. N., Thurai, M., Nakagawa, K., Huang, G. J., Kobayashi, T., Adachi, A., Hanado, H., Sekizawa, S., 2006. Rainfall estimation from C-band polarimetric radar in Okinawa, Japan: Comparison with 2D-video disdrometer and 400 MHz wind profiler, J. Meteor.

Soc. Japan, 84, 705-724.

Bringi, V. N., Williams, C. R., Thurai, M., May, P. T., 2009. Using dual-polarized radar and dual-frequency profiler for DSD characterization: A case study from Darwin, Australia. J. Atmos. Oceanic Technol. 26, 2107–2122.

Cao, Q., Zhang, G., Brandes, E., Schuur, T., Ryzhkov, A., Ikeda, K., 2008. Analysis of Video Disdrometer and Polarimetric Radar Data to Characterize Rain Microphysics in Oklahoma. J. Appl. Meteor. Climatol. 47, 2238–2255.

Cifelli, R., Williams, C. R., Rajopadhyaya, D. K., Avery, S. K., Gage, K. S., May, P. T., 2000. Drop-size distribution characteristics in tropical mesoscale convective systems. J. Appl. Meteor. 39, 760–777.

Cifelli, R., and S. A. Rutledge, 1994: Vertical motion structure in maritime continent mesoscale, convective systems: Results from 50-MHz profiler. J. Atmos. Sci., 51, 2631–2652.

Gamache, J. K., Houze Jr. R. A., Marks Jr. F. D., 1993. Dual-aircraft investigation of the inner core of Hurricane Norbert. Part III: Water budget. J. Atmos. Sci., 50, 3221–3243.

Geerts, B., Heymsfield, G. M., Tian, L., Halverson, J. B., Guillory, A., Mejia, M. I., 2000. Hurricane Georges's landfall in the Dominican Republic: Detailed airborne Doppler radar imagery. Bull. Amer. Meteor. Soc., 81, 999-1018.

Hauser, D., Amayenc, P., 1981. A new method for deducing hydrometeor-size distributions and vertical air motions from Doppler radar measurements at vertical incidence. J. Appl. Meteor. 20, 547–555.

Hu, Z., Srivastava, R. C., 1995. Evolution of raindrop size distribution by coalescence, breakup and evaporation: Theory and observations. J. Atmos. Sci., 52, 1781–1783.

Huggel, A., Schmid, W., Waldvogel, A., 1996. Raindrop Size Distributions and the Radar Bright Band. J. Appl. Meteor., 35, 1688–1701.

Atmos. Meas. Tech. Discuss., https://doi.org/10.5194/amt-2018-63
Manuscript under review for journal Atmos. Meas. Tech.
Discussion started: 12 March 2018

Jameson AR, Kostinski AB. 1998. Fluctuation properties of precipitation. Part II: reconsideration of the meaning and measurement of raindrop size distributions. J. Atmos. Sci. 55: 283–294.

Kanofsky, L., Chilson, P., 2008. An analysis of errors in drop size distribution retrievals and rain bulk parameters with a UHF wind profiling radar and a two-dimensional video disdrometer. J. Atmos. Oceanic Technol. 25, 2282–2292.

Kim, D. K., Knupp, K. R., Williams, C. R., 2009. Airflow and precipitation properties within the stratiform region of Tropical Storm Gabrielle during landfall. Mon. Wea. Rev. 137, 1954–1971.

Mapes, B. E., Houze Jr., R. A., 1995. Diabatic divergence profiles in western pacific mesoscale convective systems. J. Atmos. Sci., 52, 1807–1828.

Marks, F. D., 1985: Evolution of the structure of precipitation in Hurricane Allen (1980). Mon. Wea. Rev., 113, 909-930.

Marks, F. D., Houze, R. A., 1987. Inner core structure of Hurricane Alicia from airborne Doppler radar observations. J. Atmos. Sci., 44, 1296-1317.

Marks, F. D., Shay, L. K., USWRP PDT-5 Report, 1988. Tropical Cyclones: Forecast Problems and Associated Research Opportunities. Bull. Amer. Met. Soc., 79, 305-323.

McFarquhar, G. M., Black, R. A., 2004. Observations of particle size and phase in tropical cyclones: Implications for mesoscale modeling of microphysical processes. J. Atmos. Sci., 61, 422-439.

Liou, Y.-C., S.-F. Chang, and J. Sun, 2012: An application of the immersed boundary method for recovering the three-dimensional wind fields over complex terrain using multiple-Doppler radar data. Mon. Wea. Rev., 140, 1603-1619.

Löffler-Mang, M., and J. Joss, 2000: An optical disdrometer for measuring size and velocity

Atmos. Meas. Tech. Discuss., https://doi.org/10.5194/amt-2018-63
Manuscript under review for journal Atmos. Meas. Tech.
Discussion started: 12 March 2018

Atmospheric Measurement Techniques
Open Access
Discussions

of hydrometeors. J. Atmos. Oceanic Technol., 17, 130–139.

Lord, S. J., Willoughby, H. E., Piotrowicz, J. M., 1984. Role of a parameterized ice-phase microphysics in an axisymmetric, nonhydrostatic tropical cyclone model. J. Atmos. Sci., 41, 2836-2848.

Penide, G., A. Protat, V. Kumar, and P. T. May, 2013: Comparison of two convective/stratiform precipitation classification techniques: Horizontal reflectivity texture versus drop size distribution–based approach. *J. Atmos. Oceanic Technol.*, **30**, 2788–2797.

Powell, M. D., 1990. Boundary layer structure and dynamics in outer hurricane rainbands. Part II: Downdraft modification and mixed layer recovery. Mon. Wea. Rev., 118, 918–938.

Rajopadhyaya, D. K., May, P. T., Vincent, R. A., 1993. A general approach to the retrieval of raindrop size distributions from wind profiler Doppler spectra: Modeling results. J. Atmos. Oceanic Technol. 10, 710–717.

Rajopadhyaya, D. K., Cifelli, R. C., Avery, S. K., Williams, C. R., Ecklund, W. L., Gage, K. S., 1998. The effect of vertical air motions on rain rates and median volume diameter determined from combined UHF and VHF wind profiler measurements and comparisons with rain gauge measurements. J. Atmos. Oceanic Technol. 15, 1306–1319.

Rajopadhyaya, D. K., Avery, S. A., May, P. T., Cifelli, R. C., 1999. Comparison of precipitation estimation using single and dual-frequency wind profilers. J. Atmos. Oceanic Technol. 16, 165–173.

Joss and Waldvogel 1970. A method to improve the accuracy of radar-measured mounts of precipitation. Proc. 14th Radar Meteorology Conf., Tucson, AZ, Amer. Meteor. Soc. 237–238.

Sangren, K. L., Ray, P. S., Walker, G. B., 1984. A comparison of techniques to estimate vertical air motions and raindrop size distributions. J. Atmos. Oceanic Technol. 1, 152–165.

Schumacher C., Stevenson, S. N., Williams, C. R., (2015) Vertical motions of the tropical convective cloud spectrum over Darwin, Australia. Quarterly Journal of the Royal Meteorological Society. 141, 2277-2288.

Testud, J., S. Oury, P. Amayenc, and R. A. Black, 2001: The concept of "normalized" distribution to describe raindrop spectra: A tool for cloud physics and cloud remote sensing. J. Appl. Meteorol., 40, 1118-1140.

Tokay, A., Short, D. A., 1996. Evidence from Tropical raindrop spectra of the origin of rain from stratiform versus convective clouds. J. Appl. Meteor. 35, 355–371.

Tokay, A., Short, D. A., Williams, C. R., Ecklund, W. L., Gage, K. S., 1999. Tropical rainfall associated with convective and stratiform clouds: Intercomparison of disdrometer and profiler measurements. J. Appl. Meteor. 38, 302–320.

Tokay A, Hartmann P, Battaglia A, Gage KS, Clark WL, Williams CR. 2009. A field study of reflectivity and Z–R relations using vertically pointing radars and disdrometers. J. Atmos. Oceanic Technol. 26: 1120–1134.

Tokay. A., Wolff, D. B., Petersen, W. A., 2014. Evaluation of the new version of the laser-optical disdrometer, OTT Parsivel^2. J. Atmos. Oceanic Technol. 31, 1276–1288.

Thurai M, Bringi VN, Carey LD, Gatlin P, Schultz E, Petersen WA. 2012. Estimating the accuracy of polarimetric radar–based retrievals of drop-size distribution parameters and rain rate: an application of error variance separation using radar-derived spatial correlations. J. Hydrometeor. 13: 1066–1079.

Thurai, M., Gatlin, P. N., Bringi, V. N., 2016. Separating stratiform and convective rain types based on the drop size distribution characteristics using 2D video disdrometer data. Atmos. Res., 169, 416-423.

Ulbrich, C. W., Atlas, D., 1998. Rainfall Microphysics and Radar Properties: Analysis Methods for Drop Size Spectra. J. Appl. Meteor., 37, 912–923.

Yuter, S. E., and R. A. Houze Jr., 1997: Measurements of raindrop size distributions over the Pacific warm pool and implications for Z–R relations. J. Appl. Meteor., 36, 847–867.

Wang, D., Li, X., Tao, W.-K., Wang, Y., 2009. Effects of vertical wind shear on convective development during a landfall of severe tropical storm Bilis (2006). Atmos. Res., 94, 270-275.

Williams, C. R., Ecklund, W. L., Gage. K. S., 1995. Classification of precipitating clouds in the tropics using 915-MHz wind profilers. J. Atmos. Oceanic Technol., 12, 996-1012.

Williams, C. R., 2002. Simultaneous ambient air motion and raindrop size distributions retrieved from UHF vertical incident profiler observations. Radio Sci. 37, lO.l029/2000RS002603.

Williams, C. R., A. Kruger, K. S. Gage, A. Tokay, R. C. Cifelli, W. F. Krajewski, and C. Kummerow, 2000: Comparison of simultaneous rain drop size distributions estimated from two surface disdrometers and a UHF profiler. Geophys. Res. Lett., 27, 1763–1766.

Xu, W., Jiang, H., Kang. X., 2014. Rainfall asymmetries of tropical cyclones prior to, during, and after making landfall in South China and Southeast United States. Atmos. Res., 139, 18-26.

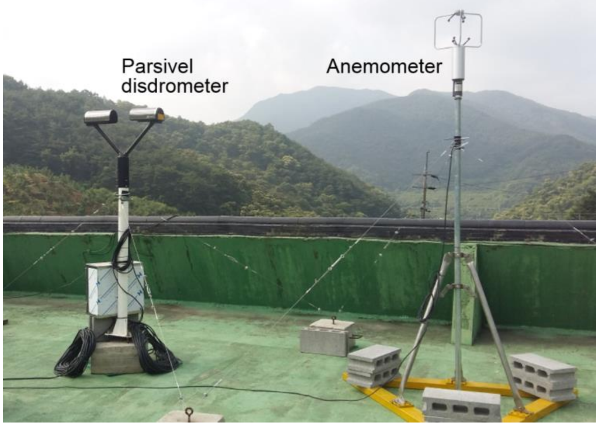

Figure 1. Picture of a Parsivel disdrometer and 3-D anemometer that were installed at a station around Mt. Jiri during the intensive observation period.

Atmos. Meas. Tech. Discuss., https://doi.org/10.5194/amt-2018-63
Manuscript under review for journal Atmos. Meas. Tech.
Discussion started: 12 March 2018

Atmospheric Measurement Techniques
Open Access
Discussions

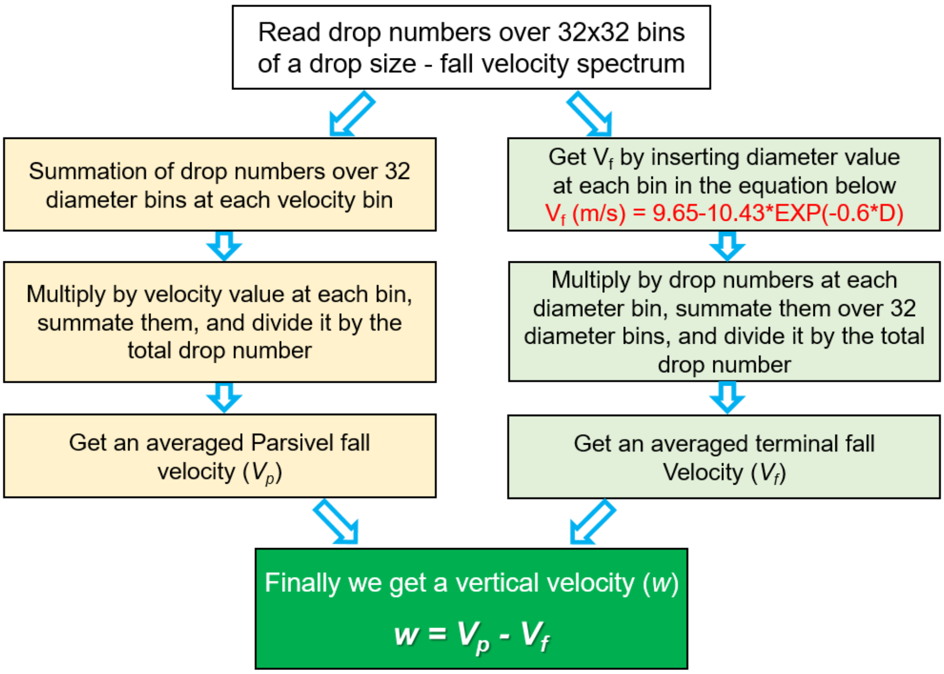

Figure 2. Flowchart for estimating w from a diameter-fall velocity spectrum of Parsivel (1-min interval). See text for more details.

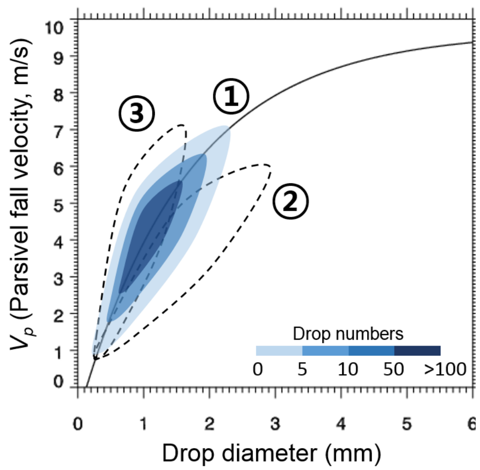

Figure 3. Schematic of Parsivel-observed diameter and fall velocity distributions for the three cases of determining zero *w*, upward *w*, and downward *w*. Contours show drop number concentrations. See text for more information.

Atmos. Meas. Tech. Discuss., https://doi.org/10.5194/amt-2018-63
Manuscript under review for journal Atmos. Meas. Tech.
Discussion started: 12 March 2018

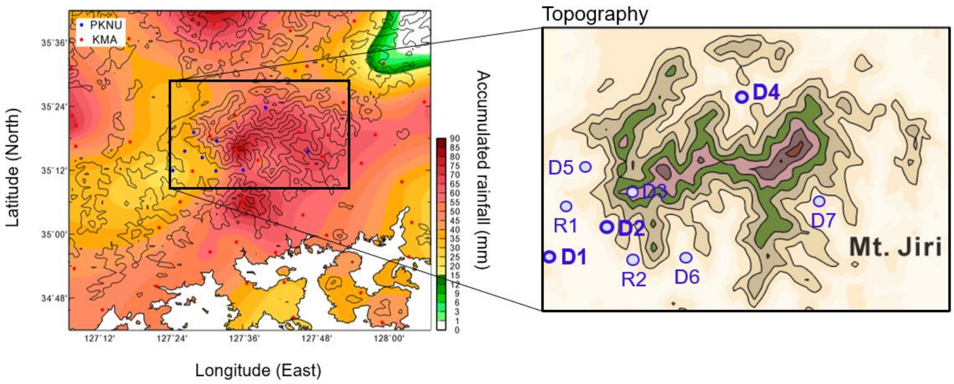

Figure 4. (a) Distribution of an acumulated rainfall (mm) on 1 July and (b) the topography of Mt. Jiri with nine observation stations. Three stations in bold are where the Parsivel and UVW measurements were analyzed in this study. R1 and R2 show stations with a rain guage only.

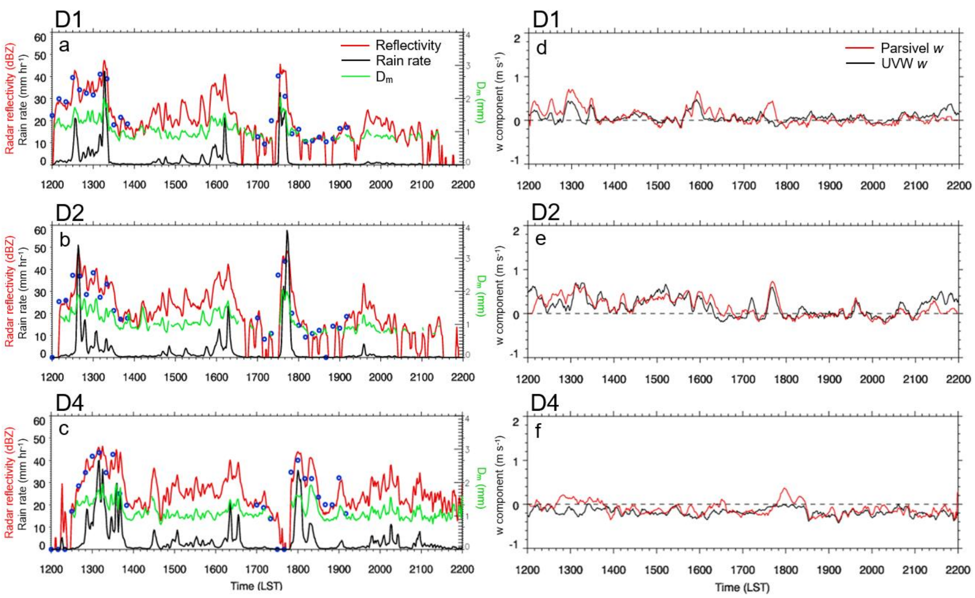

Figure 5. Time series of radar reflectivity (dBZ) in red line, rain rate (mm hr^{-1}) in black, and mass-weighted mean diameter (D_m, mm) in green at D1, D2, and D4 (left panels) and the time comparison of w_{par} (m s^{-1}) in red and w_{UVW} (m s^{-1}) in black at the same stations (right panels). Blue circles in the left panels indicate composite reflectivities (dBZ) from dual radars at the locations of D1, D2, and D4 for the selected periods.

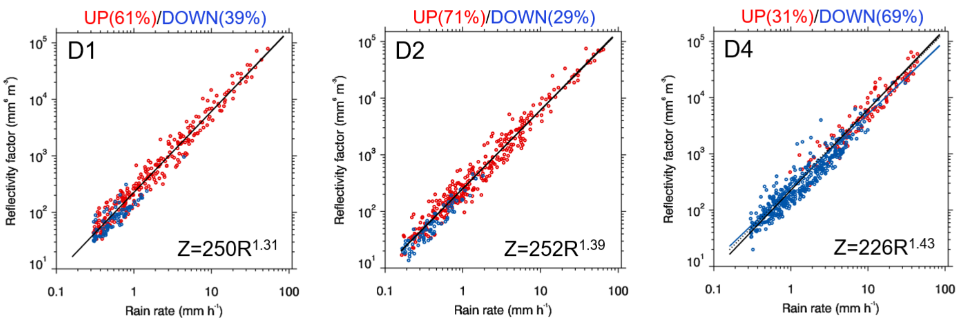

Figure 6. *Z*-*R* scatterplots at the three stations. Red dots indicate upward *w* and blue indicate downward *w*. Numbers on the top show percentages in each *w* category.

Atmos. Meas. Tech. Discuss., https://doi.org/10.5194/amt-2018-63
Manuscript under review for journal Atmos. Meas. Tech.
Discussion started: 12 March 2018

Atmospheric Measurement Techniques
Open Access
Discussions

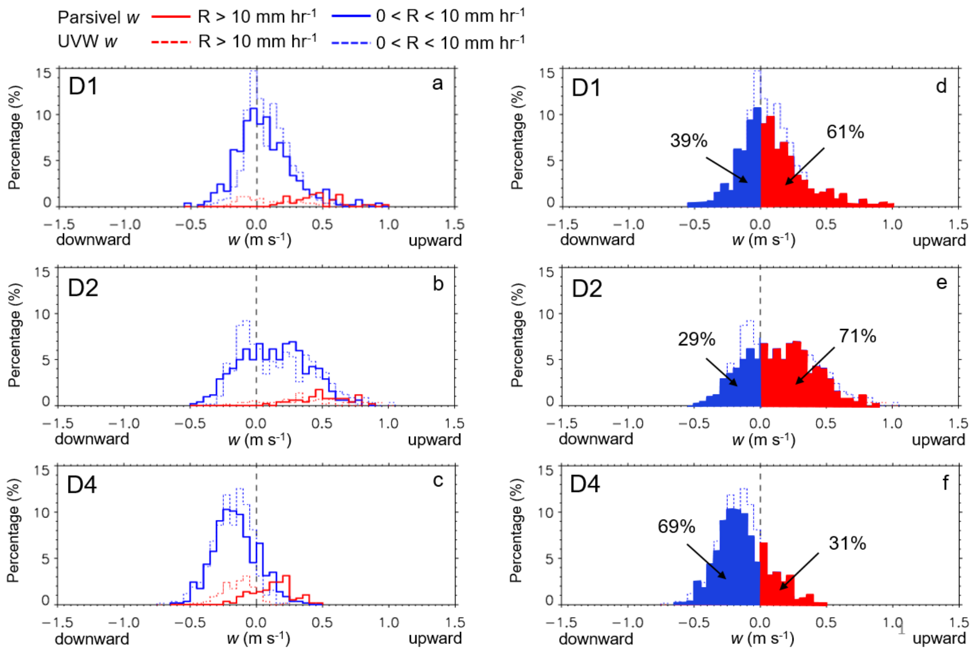

Figure 7. *w* histograms with regard to the two *R* groups (left) and those with percentages in the upward and downward *w* groups at the three stations (right).

Atmos. Meas. Tech. Discuss., https://doi.org/10.5194/amt-2018-63
Manuscript under review for journal Atmos. Meas. Tech.
Discussion started: 12 March 2018

Atmospheric Measurement Techniques
Discussions

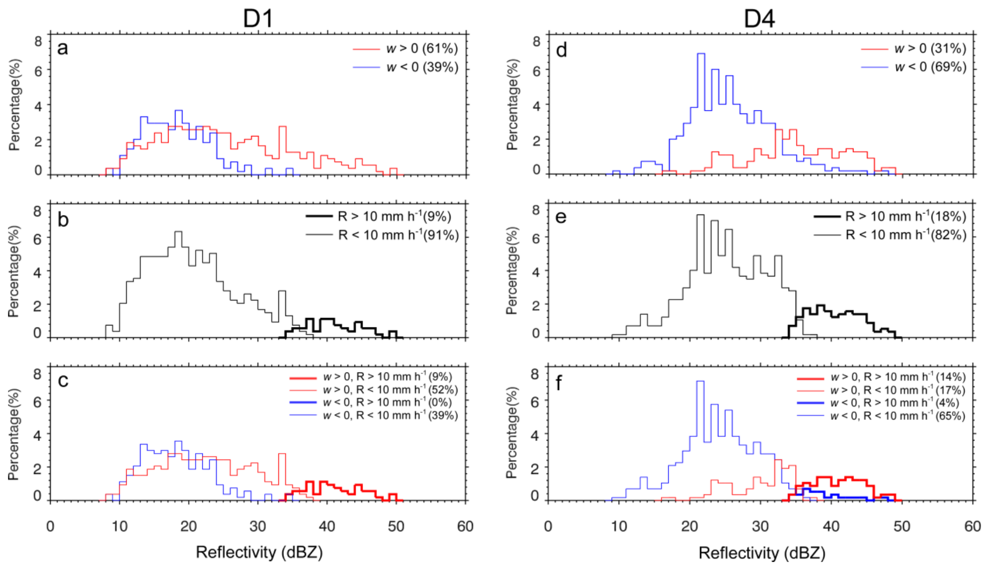

Figure 8. Z histograms with regard to w, R, and those in the four groups with percentage at D1 and D4.

Atmos. Meas. Tech. Discuss., https://doi.org/10.5194/amt-2018-63
Manuscript under review for journal Atmos. Meas. Tech.
Discussion started: 12 March 2018

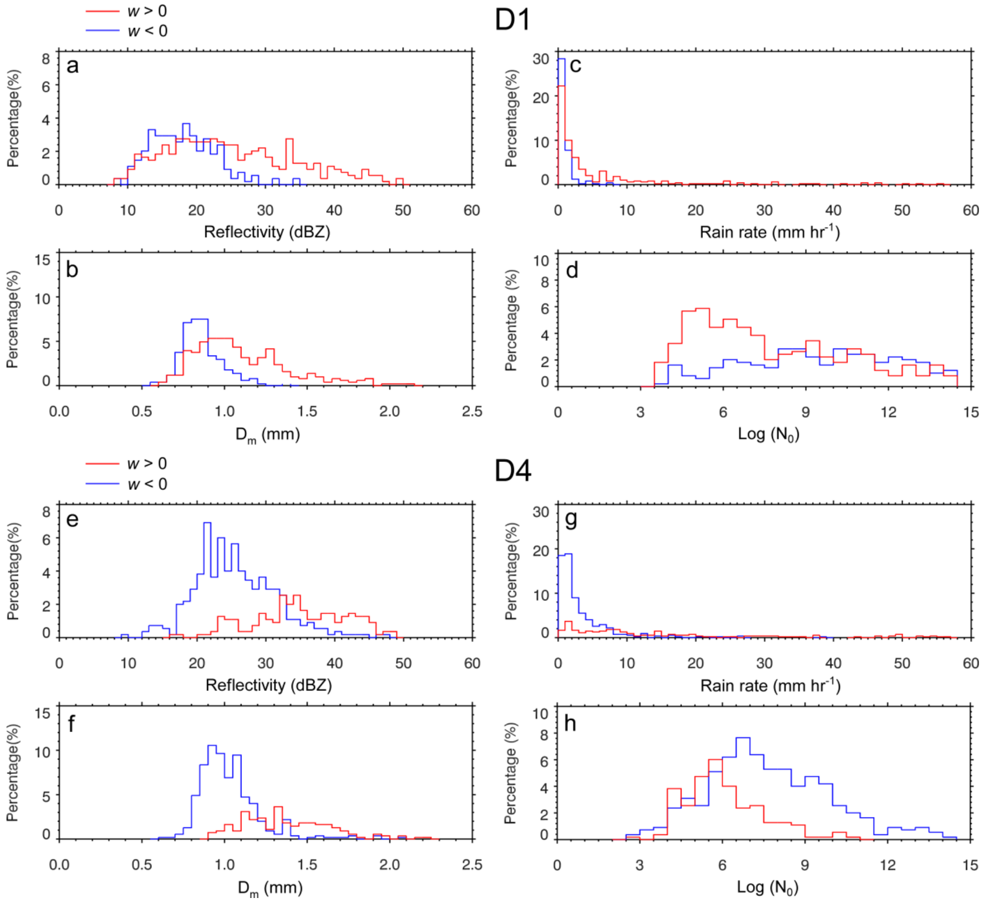

Figure 9. Histograms of retrieved DSD parameters with regard to the upward (red line) and downward *w* (blue): (a) radar reflectivity (dBZ), (b) rain rate (mm hr^{-1}), (c) D_m (mm) and (d) N_0 in log scale at D1 (top four panels) and the same as these but for D4 (bottom four panels).